Lauer, J., Olstad, B. H., Minetti, A. E., Kjendlie, P.-L., Rouard, A. H. (2015). Breaststroke swimmers moderate internal work increases toward the highest stroke frequencies. *Journal of Biomechanics, 48*, s. 3012-3016.

Breaststroke swimmers moderate internal work increases toward the highest stroke frequencies

Jessy Lauer [1,2], Bjørn Harald Olstad [1], Alberto Enrico Minetti [3], Per-Ludvik Kjendlie [1], Annie Hélène Rouard [2]

1) Department of Physical performance, Norwegian School of Sport Sciences, Oslo, Norway

2) Laboratory of Exercise Physiology (EA4338), University of Savoy, Le Bourget du Lac, France

3) Department of Pathophysiology and Transplantation, University of Milan, Milan, Italy

Keywords. Mechanical energy, swimming, predictive equation, quadrupedal locomotion.

Correspondence. LPE, Département STAPS – CISM, Bât Beaufortain, 73376 Le Bourget du Lac cedex, France. *Phone*: +33479758146. *Fax*: +33479758148.

E-mail address: jessy.lauer@gmail.com (J. Lauer)

Manuscript type. Original article.

Word count. 3236

ABSTRACT

A model to predict the mechanical internal work of breaststroke swimming was designed. It allowed us to explore the frequency–internal work relationship in aquatic locomotion. Its accuracy was checked against internal work values calculated from kinematic sequences of eight participants swimming at three different self-chosen paces. Model predictions closely matched experimental data (0.58 ± 0.07 vs 0.59 ± 0.05 J kg^{-1} m^{-1}; $t(23) = -0.30$, $P = 0.77$), which was reflected in a slope of the major axis regression between measured and predicted total internal work whose 95% confidence intervals included the value of 1 ($\beta = 0.84$, [0.61, 1.07], $N = 24$). The model shed light on swimmers ability to moderate the increase in internal work at high stroke frequencies. This strategy of energy minimization has never been observed before in humans, but is present in quadrupedal and octopedal animal locomotion. This was achieved through a reduced angular excursion of the heaviest segments (7.2 ± 2.9 and 3.6 ± 1.5 deg for the thighs and trunk, respectively, $P < 0.05$) in favor of the lightest ones (8.8 ± 2.3 and 7.4 ± 1.0 deg for the shanks and forearms, respectively, $P < 0.05$). A deeper understanding of the energy flow between the body segments and the environment is required to ascertain the possible dependency between internal and external work. This will prove essential to better understand swimming mechanical cost determinants and power generation in aquatic movements.

INTRODUCTION

While the external work (W_{ext}) refers to the work required to accelerate the body center of mass (*BCOM*), the internal work (W_{int}) reflects the work needed to accelerate a segment relative to the *BCOM*. Calculation of W_{int} is paramount to physiologists and biomechanicists. Not only does it provide a measure of internal exertion, but also allows an in-depth examination of the efficiency cascade of locomotion and the limit of the musculoskeletal system. For instance, remarkably deep insights have been gained into terrestrial gaits, unveiling the mechanical determinants of step frequency (Cavagna and Franzetti, 1986), cost of transport (Formenti et al., 2005; Minetti et al., 1994a; 1993), and gait control (Minetti et al., 1994b). It also proved clinically useful in the study of pathological gait, providing a new understanding of the role of segmental impairments in the resulting decreased economy (Detrembleur et al., 2003), and offering treatment directives in rehabilitation programs (McGibbon et al., 2001).

Despite its scientific relevance on land, such an approach remains poorly explored in human aquatic locomotion. To our knowledge, only Zamparo and colleagues computed the internal power (i.e., the amount of internal work done per unit of time) while kicking the leg (Zamparo et al., 2002; 2006) and swimming the front crawl (Zamparo et al., 2005). They found out that arm stroke internal power was rather small, contrary to the leg that occupied a great fraction (80–85%) of the total internal power. This finding was of great value since it provided a quantitative mechanical explanation of the suboptimal hydraulic efficiency of front crawl swimming (Zamparo et al., 2005).

It is striking to note how often studying the front crawl is preferred to the breaststroke in studies of aquatic locomotion. Yet breaststroke, although much less

70 economical, possesses unique features (e.g., locomotion mainly powered by the
71 synchronous action of the lower limbs, erecting trunk, glide phase) that are likely to
72 make the situation quite different compared to front crawl. It can thus serve as an
73 interesting basis to broaden our understanding of aquatic movement performance.
74 The first aim of the present study was to provide a simple predictive equation to
75 estimate the mechanical internal work of breaststroke swimming, and to check its
76 accuracy against internal work values measured from kinematic sequences captured at
77 various stroke frequencies. In a second step, it allowed us to explore the frequency–
78 internal work relationship in swimming, and contrast aquatic vs terrestrial locomotion.

MATERIAL AND METHODS

Internal work predictive equation

From the 2D analysis of Minetti (1998), mechanical internal work (in J kg^{-1} m^{-1}) during terrestrial locomotion can be predicted by the following equation:

$$W_{int} = qvf, \quad (1)$$

where q reflects the inertial properties of the moving segments, v is the average progression speed (m s^{-1}) and f the stride frequency (Hz). Later, Zamparo et al. (2002) rightly related the term v when front crawl kicking to the speed of the vertical movements of the legs. Here a similar formalism was adopted for the breaststroke distinguishing the upper and lower body anteroposterior motions. The choice to stick to a 2D approach was justified on several grounds: (1) unpublished results of internal work partitioning from our group revealed the preponderance of the work done in the sagittal plane, notably along the anteroposterior axis; (2) 3D terms would introduce more complex equations; the goal was to keep the model simple; (3) extremities can intuitively be conceived as sliding back and forth along an axis parallel to the surface. For the sake of simplicity this resembles two slider-crank mechanisms, which convert rotatory into reciprocating motion (Fig. 1): pistons (limb extremities) are animated from the center of the crankshaft (hip joint) through the cranks (thighs and trunk) and the connecting rods (lower legs and arms). Building on that analogy, the term v for the lower body motion was taken as:

$$v = 2x_{lo}\frac{f}{d_{lo}}, \quad (2)$$

given:

$$d_{lo} = 1 - t_{glide,lo} f, \quad (3)$$

where x_{lo} is the anteroposterior distance covered by the feet during half a cycle; $t_{glide,lo}$, the time the lower body spent gliding. The duty factor d_{lo} therefore expressed the fraction of the cycle duration during which the lower body is in motion relative to the *BCOM*. Without that correction, v would be greatly underestimated as leg glide—during which no W_{int} is done since legs do not move relative to the *BCOM*—would be included in the calculation. From equations (2) and (3), the internal work done by the lower body is now written:

$$W_{int,lo} = 2 q_{lo} x_{lo} \frac{f^2}{d_{lo}}. \quad (4)$$

Likewise, the internal work done by the upper body is given by:

$$W_{int,up} = 2 q_{up} x_{up} \frac{f^2}{d_{up}} \quad (5)$$

and

$$d_{up} = 1 - t_{glide,up} f, \quad (6)$$

where x_{up} refers to the anteroposterior displacement of the hands during half a cycle, and $t_{glide,up}$ is the time the upper body spent gliding. Total internal work was calculated as the sum of $W_{int,lo}$ and $W_{int,up}$. To isolate q_{lo} and q_{up}, Equations (4) and (5) can be rearranged as:

$$q_{lo} = \frac{W_{int,lo}}{2 x_{lo} \frac{f^2}{d_{lo}}} \quad (7)$$

and

$$q_{up} = \frac{W_{int,up}}{2 x_{up} \frac{f^2}{d_{up}}}. \quad (8)$$

123 *Participants and experimental validation protocol*

124

125 Eight elite Norwegian swimmers, four females (19.3 ± 6.1 years; 1.69 ± 0.04 m; 65.6
126 ± 5.2 kg) and four males (25.0 ± 3.1 years; 1.90 ± 0.03 m; 88.0 ± 2.5 kg) volunteered
127 to participate in this study. Before participation, they signed informed consent forms
128 approved by the Norwegian national ethics committee. Tests took place in a 25-m
129 indoor swimming pool. After a 15-min warm-up consisting of low- to moderate-
130 intensity aerobic swimming, each participant swam three 25-m breaststroke laps at
131 different self-chosen paces and stroke frequencies interspersed with 2-min rest
132 periods.

133

134 *Kinematic analysis*

135

136 Kinematic data were obtained by tracking 3D marker positions using the motion
137 capture technique (Qualisys Track Manager 2.6, Qualisys, Gothenburg, Sweden). Ten
138 cameras (Oqus 3 and 4 series, 100 Hz) were placed in waterproof cases, six of them
139 mounted just below the water surface and four standing on tripods at the bottom of the
140 pool. They were calibrated using a wand with two markers (inter-point distance 749.5
141 mm), moved in a volume of about 37.5 m^3, 10 m (*X*; pointing horizontally and in the
142 sense of forward motion) × 2.5 m (*Y*; horizontally and laterally towards the left of the
143 swimmer) × 1.5 m (*Z*; vertically and dorsally) so that each camera covered at least
144 800–1000 points. The root mean square reconstruction error for position was 1.6 mm.
145 The body was modeled as 13 rigid segments (feet, shanks, thighs, hands,
146 forearms, upper arms, and trunk) according to de Leva (1996). Twenty-seven retro-
147 reflective markers—19 mm in diameter, developed to suit underwater usage—were

148 thus positioned on each body side as follows: acromion, lateral epicondyle, great
149 trochanter, lateral femoral condyle, calcaneus, lateral malleolus, first and fifth
150 metatarsophalangeal joint, a three-marker cluster on the hand (dorsal wrist, second
151 and fifth metacarpophalangeal joints). To later reconstruct segment six degrees of
152 freedom, four additional four-marker clusters were placed laterally on the forearm,
153 upper arm, thigh and shank according to the directions provided by Cappozzo et al.
154 (1997).

155 MATLAB R2013a (The MathWorks, Inc. Natick, MA, USA) was used for data
156 processing. Marker coordinates were filtered using the singular spectrum analysis
157 (Alonso et al., 2005): the fourth main components were retained for signals
158 reconstruction and a window length of $l/10$ was chosen, with l being the length of the
159 time series (Ishimura and Sakurai, 2012). One stroke cycle per participant was
160 analyzed in the middle of the pool when swimming speed is stabilized. A cycle was
161 defined between two consecutive starting backward movements of the heels.
162 Respective segment masses, center of mass (*COM*) locations and moments of inertia
163 were estimated for both male and females from de Leva's anthropometric tables
164 (1996). The coordinates of the *BCOM* were determined for each frame from the
165 masses and the instantaneous positions of each of the 13 segments *COM*s.

166

167 *Mechanical internal work calculation*

168

169 *BCOM* velocity was calculated as the first derivative of its position with respect to
170 time. The linear velocity of the *COM* of each segment relative to the *BCOM* was
171 obtained in the same way, from differentiation of the difference between the absolute
172 coordinates of segment *COM* and those of the *BCOM*. Each set of axes was made

orthonormal (correcting unit floating axes by two successive cross-products), and defined a local, right-handed reference frame centered on the segment *COM* (Cappozzo et al., 2005). Segment 3D orientation in space was represented by unit quaternions (a way to parameterize rigid body attitude that does not suffer from singularities, unlike traditional Euler angles), and angular velocity components derived from quaternion rates (Diebel, 2006). At a later stage, segment angles were projected onto the sagittal plane, the minimum and maximum values determined, and the angular excursion calculated.

The internal energy level (E_{int}) of a system of n segments of mass m at instant t can be expressed as:

$$E_{\text{int}}(t) = \sum_{i=1}^{n} \left(\underbrace{\frac{1}{2} m_i \left(v_{xti}^2 + v_{yti}^2 + v_{zti}^2 \right)}_{E_{\text{k,t}}} + \underbrace{\frac{1}{2} \left(I_{xi} \omega_{xti}^2 + I_{yi} \omega_{yti}^2 + I_{zi} \omega_{zti}^2 \right)}_{E_{\text{k,r}}} \right), \tag{9}$$

where v is the linear velocity of the *COM* of the ith segment relative to the *BCOM*; ω and I, the angular velocity and moment of inertia of the ith segment around the principal axes (x, longitudinal axis; y, transverse axis; z, sagittal axis). The first term of the sum refers to the translational kinetic energy, while the second yields the rotational kinetic energy (respectively, $E_{\text{k,t}}$ and $E_{\text{k,r}}$).

In order to yield realistic internal work values, kinetic energy transfers should be included in the analysis (Willems et al., 1995). Accordingly, kinetic energy curves were summed among adjacent segments within a same limb only in order to exclude energy transfers through the *BCOM* from one limb to another that are not likely to occur. Increments in the resulting traces were then summed, and yielded the positive work to accelerate the segments relative to the *BCOM*. The total internal work W_{int}

was expressed as J per kg of body mass and unit distance (m) travelled, a customary unit for the mechanical cost of locomotion.

Statistical analysis

STATA 12 (StataCorp, Inc., College Station, TX, USA) was used for all analyses, and the critical significance level set at 0.05. Data are expressed as means ± SD. Normal Gaussian distribution was checked for all variables by the Shapiro–Wilk test prior to analysis. The mean measured internal work was compared with the mean predicted internal work using the Student's paired *t*-test. Whether the theoretical predictions and the measurements deviated from identity was assessed with a major axis regression. The model was considered perfectly accurate if the 95% confidence interval of the slope β of the major axis included a value of 1 (Rayner, 1985). Differences in angular excursion between the lowest and highest frequencies were tested for a statistical difference from 0 using one-sample *t*-tests.

RESULTS

Stroke frequencies measured in the present study ranged from 0.50 to 0.77 Hz, corresponding to swimming speeds within the interval 0.82–1.18 m s^{-1}. Increased stroke frequency was associated with enhanced swimming speed (females: $r(10) = 0.92$, $P < 0.001$; males: $r(10) = 0.84$, $P = 0.006$). Values of internal work predicted by the model were remarkably close to the experimental data (0.58 ± 0.07 vs 0.59 ± 0.05 J kg^{-1} m^{-1}; $t(23) = -0.30$, $P = 0.77$; Fig. 2). This was reflected in a slope of the major axis regression between measured and predicted total internal work whose 95% confidence intervals included the value of 1 ($\beta = 0.84$, [0.61, 1.07], $N = 24$). Internal work increased linearly as stroke frequency rose (Fig. 3, upper panel). Neither duty factors d_{lo} and d_{up} ($r(22) = -0.03$, $P = 0.90$; $r(22) = -0.05$, $P = 0.82$, respectively; Fig. 3, second panel) nor limbs anteroposterior displacement x_{lo} and x_{up} correlated with stroke frequency ($r(22) = -0.06$, $P = 0.77$; $r(22) = 0.08$, $P = 0.55$, respectively; Fig. 3, third panel), whereas q_{lo} and q_{up} correlated negatively with stroke frequency ($r(22) = -0.86$, $P < 0.001$; $r(22) = -0.68$, $P < 0.001$, respectively; Fig. 3, lower panel).

All segments but the upper arm exhibited significant differences in angular excursion between the laps swum at the highest frequency and those at the lowest (Fig. 4). Angular excursion was significantly increased at the shank (8.8 ± 2.3 deg, $P = 0.007$) and at the forearm (7.4 ± 1.0 deg, $P = 0.038$). Conversely, angular excursion was reduced at the thigh (7.2 ± 2.9 deg, $P = 0.041$) and at the trunk (3.6 ± 1.5 deg, $P = 0.048$).

DISCUSSION

Our 2D model was straightforward, yet accurate in predicting changes in 3D breaststroke swimming internal work. These successful predictions suggest that motion along the mediolateral axis can safely be disregarded; the sagittal plane alone provided satisfactory information. Furthermore, modeling upper and lower body motions as two piston mechanisms was a sound approach to capture breaststroke dynamics. Linear velocities of the extremities in both breaststroke and slider-crank systems rightly reflect the speed at which the whole chain is animated. As such, hand and feet motions along the anteroposterior axis are good markers of W_{int} done during aquatic locomotion.

Our results revealed that upper and lower body had equal and constant duty cycles, and similar downward trends in the parameter q. The model can hence be made simpler setting $d_{lo} = d_{up} = 0.5$ and $q = q_{lo} = q_{up}$, and writes: $W_{int} = 4qf^2\left(x_{lo} + x_{up}\right)$. The sum of the upper and lower body anteroposterior displacement being invariant (1.07 ± 0.02 m; see Fig. 3, third panel), replacing now gives: $W_{int} = 4.28qf^2$. Regressing q against f, we obtain $q = -0.72f + 0.81$, which, fed back into the previous equation, yields: $W_{int} = -3.08f^3 + 3.47f^2$. This latter model tended to slightly underestimate measured internal work (0.58 ± 0.05 vs 0.60 ± 0.07, $t(23)$ = -0.41, P = 0.69), with major axis slope 95% confidence intervals excluding 1 though (β = 0.61, [0.42, 0.81], N = 24). More importantly, however, as the model only requires the input of stroke frequency (which can be readily measured), it remained entirely satisfactory whenever underwater camera set-up is unavailable.

256 The compound term q accounts for limb geometry and inertial properties
257 (Minetti, 1998; Nardello et al., 2011). Here this parameter was found to decline as the
258 stroke frequency (and the swimming speed) increased. According to Minetti (1998), a
259 decrease in q conveys the ability to minimize the locomotion mechanical work by
260 reducing the moment needed to rotate the limbs. This capacity has never been
261 observed before in humans, q being constant in walking, running (Minetti, 1998;
262 Nardello et al., 2011) and cycling (Minetti et al., 2001). However, it exists in horses
263 (Minetti, 1998) and spiders (Biancardi et al., 2011). Quadrupeds and octopods
264 essentially contrast with bipeds in that they display higher stability and more versatile
265 locomotor repertoire. While human limb geometry is constrained either during the
266 walking and running stance phase or by the crank length while pedaling, horses
267 passing from walk to trot show remarkable changes in limb geometry (Minetti, 1998).
268 Likewise, spiders exhibit distinct limb motion patterns between low and high stride
269 frequencies (Biancardi et al., 2011). Breaststroke swimmers therefore resemble, from
270 the point of view of locomotion dynamics, quadrupeds demonstrating different gaits.
271 The aquatic environment, lacking solid support unlike on land, provides additional
272 freedom in limb movement. In breaststroke, a trade-off could exist between
273 'grouping' the lower body segments near the *BCOM* before the kick (possibly
274 lessening W_{int}) and the higher hydrodynamic resistance that this would entail.
275 Hogan (1985) advanced that the central nervous system may alter the inertial
276 behavior of a multi-joint limb by changing its configuration in space, thanks to
277 additional degrees of freedom provided by the kinematic redundancy of the skeletal
278 system. Here we found that all segments but the upper arm had significantly different
279 angular excursions between the highest and the lowest movement frequency.
280 Specifically, the angular excursions of the heaviest segments (thighs and trunk) were

281 reduced with increased frequency, and vice versa for the lightest segments (shanks
282 and forearms). This finding is in agreement with the 'Knowledge II' theory of the
283 planning and control of motor action (Rosenbaum et al., 1995). It indeed predicts the
284 apportionment of lower amount of motion by the central nervous system to segments
285 with high inertia, while segments with low inertia would exhibit an increase or a
286 much smaller decrease in angular amplitude. Since the anteroposterior displacement
287 for both upper and lower body was constant regardless of swimming frequency,
288 favoring lighter segments toward the highest frequencies contributed to the decrease
289 in q. Swimmers thus proved able to reduce the moment needed to rotate their limbs
290 through motor reorganization, therefore slowing down the increase in internal work.

291 An additive, hypothetical mechanism contributing to decrease the internal work
292 needed may rest on the added mass concept from fluid mechanics. As the velocity of a
293 body is changing in water, the rate of change of kinetic energy of the fluid is changing
294 also. This amount of energy is regarded as arising from a mass of fluid added to the
295 mass of the body (Batchelor, 1967). It should be emphasized that this distinct mass of
296 water is rather virtual: in fact, every fluid particle will accelerate to varying degrees as
297 the body moves, the added mass being a weighted integration of this entire mass
298 (Newman, 1999). The body behaves as if it was heavier, and additional mechanical
299 work is required against both the inertia of the body itself and the inertia of the
300 displaced fluid (Brennen, 1982). At the surface—where swimmers actually are—there
301 is no such a simple physical interpretation. Fluid mechanics studies of cylinders
302 oscillating at the surface offer a clear illustration. Under a certain range of oscillation
303 frequencies, free surface deformations have been found to yield decreasing or even
304 negative added masses (Chung, 1977; Frank, 1967). And it is incorrect to interpret a
305 negative added mass as a subtracted mass of water (Falnes, 1983). These surprising

findings may be explained on the basis of a standing wave system resonating above the body (Newman et al., 1984). In that ideal case, the wave energy flux is zero; no additional external work is needed to deform the free surface, hence the work to overcome inertia is less. Similar hydrodynamic interference effects might as well occur in breaststroke swimming. Sanders et al. (1998) did not support a posteriorly travelling wave in breaststroke; perhaps counter-propagating waves are created by the oscillating trunk and lower limbs, approaching a resonant system as swimming frequency increases. Reduced added mass by this means would contribute to decrease the work required to accelerate the segments relative to the *BCOM*.

Our understanding of the relationship between W_{int} and W_{ext} in aquatic locomotion is impeded by the lack of attention being paid to added mass and wave generation. Costs of moving the segments relative to the body center of mass, and of imparting kinetic energy to the water have been regarded in the past as two independent, additive components within the energy cascade in aquatic locomotion (Zamparo et al., 2002). Based on the above, the two might actually be coupled to some extent. In effect, a decelerating segment will generate extra thrust due to the added mass inertia (Vogel, 1994). Thus, as pointed out by Kautz and Neptune (2002) in cycling, internal energy decreases might ultimately produce positive external work in swimming also.

CONCLUSION

A simple yet accurate predictive equation was devised to estimate the internal work of breaststroke swimming. This is a valuable component of a more comprehensive model including W_{ext}, which would predict the metabolic energy expenditure associated to a given speed and stroke frequency in breaststroke swimming. It shed

light on swimmers ability to moderate the increase in W_{int} at the highest stroke frequencies. Such capacity, never observed before in humans, is also present in quadrupedal and octopedal animal locomotion. This was achieved through a reduced angular excursion of the heaviest segments in favor of the lightest ones. Perhaps W_{int} is sensed and triggers such motor responses. A deeper understanding of the energy flow between the body segments and the environment is required to ascertain the possible dependency between W_{int} and W_{ext}. Considering added mass and wave concepts will prove essential to better understand swimming cost determinants and power generation in aquatic movements.

CONFLICT OF INTEREST STATEMENT

The authors declare no conflict of interest.

REFERENCES

Alonso, F.J., Castillo, J.M.D., Pintado, P., 2005. Application of singular spectrum analysis to the smoothing of raw kinematic signals. J Biomech 38, 1085–1092.

Batchelor, G.K., 1967. An Introduction to Fluid Dynamics. Cambridge University Press, Cambridge, UK.

Biancardi, C.M., Fabrica, C.G., Polero, P., Loss, J.F., Minetti, A.E., 2011. Biomechanics of octopedal locomotion: kinematic and kinetic analysis of the spider Grammostola mollicoma. J Exp Biol 214, 3433–3442.

Brennen, C.E., 1982. A review of added mass and fluid inertial forces. (No. CR82.010). Naval Civil Engineering Laboratory, Port Hueneme, CA.

Cappozzo, A., Cappello, A., Croce, Della, U., Pensalfini, F., 1997. Surface-marker cluster design criteria for 3-D bone movement reconstruction. IEEE Trans Biomed Eng 44, 1165–1174.

Cappozzo, A., Croce, Della, U., Leardini, A., Chiari, L., 2005. Human movement analysis using stereophotogrammetry. Part 1: theoretical background. Gait Posture 21, 186–196.

Cavagna, G.A., Franzetti, P., 1986. The determinants of the step frequency in walking in humans. J Physiol 373, 235–242.

Chung, J.A.F., 1977. Forces on submerged cylinders oscillating near a free surface. Journal of Hydronautics 11, 100–106.

de Leva, P., 1996. Adjustments to Zatsiorsky-Seluyanov's segment inertia parameters. J Biomech 29, 1223–1230.

Detrembleur, C., Dierick, F., Stoquart, G., Chantraine, F., Lejeune, T., 2003. Energy cost, mechanical work, and efficiency of hemiparetic walking. Gait Posture 18, 47–55.

Diebel, J., 2006. Representing Attitude: Euler Angles, Unit Quaternions, and Rotation Vectors, Matrix.

Stanford University, Stanford, CA.
Falnes, J., 1983. Added-mass matrix and energy stored in the “near field.” Universitetet i Trondheim, Noregs tekniske høgskole, Institutt for eksperimentalfysikk, Trondheim, Norway.
Formenti, F., Ardigò, L.P., Minetti, A.E., 2005. Human locomotion on snow: determinants of economy and speed of skiing across the ages. Proc Biol Sci 272, 1561–1569.
Frank, W., 1967. Oscillation of cylinders in or below the free surface of deep fluids. Naval Ship Research and Development Center, Washington.
Hogan, N., 1985. The mechanics of multi-joint posture and movement control. Biol Cybern 52, 315–331.
Ishimura, K., Sakurai, S., 2012. Effect of window length when smoothing with singular spectrum analysis technique in running data. In: Bradshaw, E.J., Burnett, A., Hume, P.A. (Eds.), Proceedings of the XXXth International Conference on Biomechanics in Sports. Australian Catholic University, Melbourne, Australia, pp. 29–32.
Kautz, S.A., Neptune, R.R., 2002. Biomechanical determinants of pedaling energetics: internal and external work are not independent. Exerc Sport Sci Rev 30, 159–165.
McGibbon, C.A., McGibbon, C.A., Krebs, D.E., Krebs, D.E., Puniello, M.S., Puniello, M.S., 2001. Mechanical energy analysis identifies compensatory strategies in disabled elders' gait. J Biomech 34, 481–490.
Minetti, A.E., 1998. A model equation for the prediction of mechanical internal work of terrestrial locomotion. J Biomech 31, 463–468.
Minetti, A.E., Ardigò, L.P., Saibene, F., 1993. Mechanical determinants of gradient walking energetics in man. J Physiol 472, 725–735.
Minetti, A.E., Ardigò, L.P., Saibene, F., 1994a. Mechanical determinants of the minimum energy cost of gradient running in humans. J Exp Biol 195, 211–225.
Minetti, A.E., Ardigò, L.P., Saibene, F., 1994b. The transition between walking and running in humans: metabolic and mechanical aspects at different gradients. Acta Physiol Scand 150, 315–323.
Minetti, A.E., Pinkerton, J., Zamparo, P., 2001. From bipedalism to bicyclism: evolution in energetics and biomechanics of historic bicycles. Proc Biol Sci 268, 1351–1360.
Nardello, F., Ardigò, L.P., Minetti, A.E., 2011. Measured and predicted mechanical internal work in human locomotion. Hum Mov Sci 30, 90–104.
Newman, J.N., 1999. Marine Hydrodynamics, 9 ed. The MIT Press, Cambridge, MA.
Newman, J.N., Sortland, B., Vinje, T., 1984. Added mass and damping of rectangular bodies close to the free surface. Journal of Ship Research 28, 219–228.
Rayner, J.M.V., 1985. Linear relations in biomechanics: the statistics of scaling functions. J Zool 206, 415–439.
Rosenbaum, D.A., Loukopoulos, L.D., Meulenbroek, R.G., Vaughan, J., Engelbrecht, S.E., 1995. Planning reaches by evaluating stored postures. Psychol Rev 102, 28–67.
Sanders, R.H., Cappaert, J.M., Pease, D.L., 1998. Wave characteristics of olympic breaststroke swimmers. J Appl Biomech 14, 40–51.
Vogel, S., 1994. Life in Moving Fluids: The Physical Biology of Flow. Princeton University Press, Princeton, NJ.
Willems, P.A., Cavagna, G.A., Heglund, N.C., 1995. External, internal and total work in human locomotion. J Exp Biol 198, 379–393.
Zamparo, P., Pendergast, D.R., Mollendorf, J.C., Termin, A.C., Minetti, A.E., 2005. An energy balance of front crawl. Eur J Appl Physiol 94, 134–144.
Zamparo, P., Pendergast, D.R., Termin, B., Minetti, A.E., 2002. How fins affect the economy and efficiency of human swimming. J Exp Biol 205, 2665–2676.
Zamparo, P., Pendergast, D.R., Termin, A., Minetti, A.E., 2006. Economy and efficiency of swimming at the surface with fins of different size and stiffness. Eur J Appl Physiol 96, 459–470.

421 **FIGURE CAPTIONS**

422 Fig. 1. A breaststroke swimmer modeled as two slider-crank mechanisms. Extremities
423 are sliding back and forth along an axis (dash line) parallel to the surface, and
424 animated from the center of the crankshaft (hip joint) through the cranks (thighs and
425 trunk) and the connecting rods (lower legs and arms).

426

427 Fig. 2. Predicted against measured mechanical internal work. The dotted line is the
428 identity line. The major axis computed for the full body predictions is not represented.
429 Dots are individual internal work values computed from 24 kinematic sequences at
430 various speed and frequencies (white: upper body; grey: lower body; filled: full
431 body).

432

433 Fig. 3. The upper panel displays the measured internal work as a function of stroke
434 frequency. The second panel reports the duty cycle values for upper and lower body.
435 The third panel illustrates the horizontal displacements of upper and lower body, and
436 the lower panel shows the parameter q—reflecting the inertial properties of the
437 moving segments—obtained from Eqs 7 and 8. Dot colors are as in Fig. 2.

438

439 Fig. 4. Differences in segment angular excursion between the highest and lowest
440 stroke frequencies (mean ± SD). Positive values indicate an increased sweep angle in
441 the vertical plane, and vice versa. Constant horizontal displacements of upper and
442 lower body were achieved, toward the highest frequencies, through a reduction of
443 angular excursion of the heaviest segments (thighs and trunk) in favor of the lightest
444 ones (shanks and forearms). * Significantly different from 0 ($P < 0.05$).

445

446 **FIGURES**

447 **Figure 1**

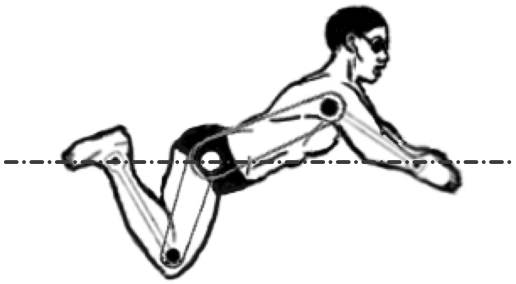

448

449 **Figure 2**

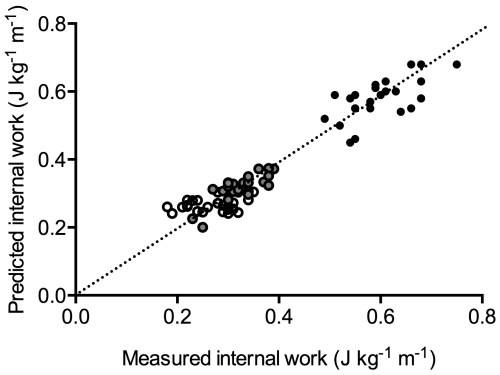

450

451 **Figure 3**

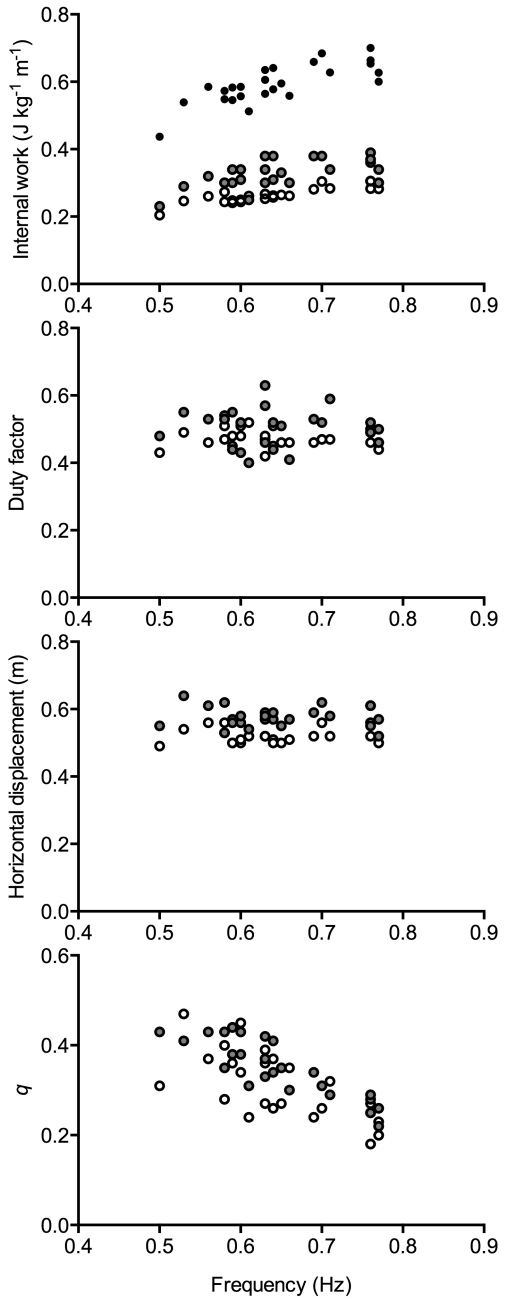

452

453 **Figure 4**

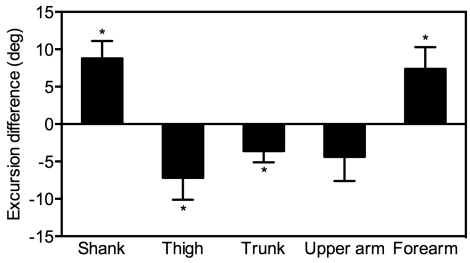

454